7-12-2021

Temperature dependence of field-response mechanisms in $0.4Ba(Zr_{0.2}Ti_{0.8})O_3$-$0.6(Ba_{0.7}Ca_{0.3})TiO_3$

Chris M. Fancher
Oak Ridge National Laboratory

Özgür Keleş
San Jose State University, ozgur.keles@sjsu.edu

Matthias Ehmke
Purdue University

Keith J. Bowman
University of Maryland, Baltimore County (UMBC)

Recommended Citation

Chris M. Fancher, Özgür Keleş, Matthias Ehmke, and Keith J. Bowman. "Temperature dependence of field-response mechanisms in $0.4Ba(Zr_{0.2}Ti_{0.8})O_3$-$0.6(Ba_{0.7}Ca_{0.3})TiO_3$" *Applied Physics Letters* (2021). https://doi.org/10.1063/5.0056110

Applied Physics Letters

RESEARCH ARTICLE | JULY 14 2021

Temperature dependence of field-response mechanisms in $0.4Ba(Zr_{0.2}Ti_{0.8})O_3–0.6(Ba_{0.7}Ca_{0.3})TiO_3$

Chris M. Fancher ✉; Özgür Keleş; Matthias Ehmke; ... et. al

Appl. Phys. Lett. 119, 022904 (2021)
https://doi.org/10.1063/5.0056110
CHORUS

AIP Publishing

Applied Physics Letters ARTICLE scitation.org/journal/apl

Temperature dependence of field-response mechanisms in $0.4Ba(Zr_{0.2}Ti_{0.8})O_3$–$0.6(Ba_{0.7}Ca_{0.3})TiO_3$

Cite as: Appl. Phys. Lett. **119**, 022904 (2021); doi: 10.1063/5.0056110
Submitted: 6 May 2021 · Accepted: 26 June 2021 ·
Published Online: 14 July 2021

Chris M. Fancher,[1,2,a)] Özgür Keleş,[3] Matthias Ehmke,[4] and Keith J. Bowman[5]

AFFILIATIONS

[1]Material Science and Technology Directorate, Oak Ridge National Laboratory, Oak Ridge, Tennessee 37830, USA
[2]Neutron Scattering Division, Oak Ridge National Laboratory, Oak Ridge, Tennessee 37830, USA
[3]Chemical and Materials Engineering Department, San Jose State University, San Jose, California 95192, USA
[4]School of Materials Engineering, Purdue University, West Lafayette, Indiana 47907, USA
[5]College of Engineering and Information Technology, University of Maryland Baltimore County, Baltimore, Maryland 21250, USA

[a)]**Author to whom correspondence should be addressed:** fanchercm@ornl.gov

ABSTRACT

Understanding the temperature dependence of how ferroelectric materials respond to electric fields is critical for determining how best to use these materials in applications. Here, temperature dependent *in situ* x-ray diffraction is used to study how field-response mechanism $Ba(Zr_{0.2}Ti_{0.8})O_3$–$x(Ba_{0.7}Ca_{0.3})TiO_3$ evolves with temperature. Increasing the measurement temperature was found to slightly reduce the extent of domain reversal and the magnitude of the 111 lattice strain. Instead, these results indicate that temperature predominantly impacted the angular dependence of the 002/200 lattice strain. We attribute the observed differences in 002/200 lattice strain to the flattening of the free-energy near the tetragonal-orthorhombic phase boundary, where the flattening of the energy landscape promotes a polarization rotation response during the application of electric fields at room temperature.

Piezoceramics are widely used in a variety of applications (e.g., actuator, sensor, fuel injection, micropositioning, and ultrasound imaging).[1] The functional properties of piezoceramics have enabled device miniaturization and novel device funcationality.[2] Lead-based material systems have dominated the growth in the use of piezoceramics due to their attractive electromechanical properties.[3,4] Concerns over the potential negative impact from the processing, use, and/or waste of lead-based materials on the environment have resulted in governments imposing restrictions on their use.[5] Government regulations challenged the scientific community to identify novel lead-free systems that achieve or surpass the functional properties of today's state-of-the-art lead-based systems.[6] In 2004, Saito *et al.* used a combination of chemical doping and templated grain growth to demonstrate the viability of lead-free piezoceramics by achieving an electromechanical performance in $K_{1/2}Na_{1/2}NbO_3$ that matched lead-based ceramics.[7] This finding, combined with the threat of government regulations, sparked a nearly decade and a half search for lead-free alternatives.[6]

Of the lead-free systems, $BaTiO_3$ (BT)-based ceramics have shown promise as potential lead-free replacements for actuator and dielectric applications.[8–10] Research has shown that BT is an ideal host for solid-solution tuning of the electromechanical and dielectric properties.[11] Incorporation of $BiZn_{1/2}Ti_{1/2}O_3$ into BT stabilizes a high dielectric response over a wide temperature range by destabilizing the local atomic configuration.[12] Solid-solutioning has proven a viable route for enhancing the piezoelectric response of BT-based materials with $Ba(Zr_{0.2}Ti_{0.8})O_3$–$x(Ba_{0.7}Ca_{0.3})TiO_3$ (BZT-BCT) being one of the most promising candidates.[13] BZT-BCT has been shown to achieve a large signal (d^*_{33}) of >1500 pm/V with a 10 MPa prestress, making it well suited for low temperature (<100 °C) actuator applications.[14] One drawback of BZT-BCT is that the electromechanical properties are strongly dependent on temperature.[15] The high BCT tetragonal region of the phase diagram exhibits the best thermal stability.

The present study investigates the temperature dependence of the field-response mechanisms (e.g., ferroelectric/ferroelastic domain reorientation and lattice strain) in tetragonal BZT-60BCT by *in situ* x-ray diffraction. Diffraction data were measured during the application of electric fields at room temperature and 56 °C. These data

highlight that the extent of both lattice strain and domain reorientation are slightly reduced at elevated temperatures. These results suggest that the observed differences in the field responses are a direct consequence of the shift in morphotropic phase boundary (MPB) composition with temperature, where increasing temperature reduces the extrinsic contributions associated with the proximity to ferroelectric–ferroelectric tetragonal-orthorhombic (T-O) polymorphic phase boundary (PPB). BZT-BCT piezoelectric ceramics with $x = 0.6$ BCT (herein referred to as 60BCT) were prepared using conventional powder processing. See Ref. 16 for further details about ceramic processing. Compacted disks were sintered at 1300 °C for 4 h and had an average grain size of $19 \pm 4\,\mu$m. Sintered disks were cut into rectangular cuboid specimens ($0.8 \times 1 \times 7$ mm), and silver electrodes were painted on opposite 1×7 mm sides. X-ray diffraction (XRD) data were measured *in situ* during the application of electric fields at beamline 11IDC of the Advanced Photon Source at Argonne National Laboratory. Data were measured in transmission geometry as schematically shown in Fig. 1. A monochromatic $500 \times 500\ \mu m^2$ beam of 0.11165 Å x-rays (111 keV) was used for the diffraction experiment. A hot air blower was used to heat the silicon oil bath used to mitigate dielectric breakdown along the edge of the sample. The temperature was measured using a thermocouple submerged in the silicone oil bath. Diffraction images were measured every 0.4 s during the application of bipolar triangular waveform (20 s period) of the maximum amplitude of 3.0 kV/mm using a Perkin Elmer flat-panel two-dimensional detector. Samples were rocking 5° in chi and omega to improve the orientation average of the measured data. Measured diffraction images were reduced into intensity vs scattering angle for grains with their scattering vectors oriented 0, 54, and 90° from the applied field with a ± 15° integration width using the software package pyFAI.[17]

The application of electric fields induces both lattice strain and domain wall motion (DWM) in 60BCT, which provides intrinsic and extrinsic contributions to the macroscopic strain response. Electric field-dependent XRD of the 111 and 002/200 measured RT and 56 °C are shown in Fig. 2. See Fig. S1 for a comparison of the angular-dependent data. These data are qualitatively similar, with extensive 111 peak shifts and intensity interchange between the 002 and 200 observed in both datasets. Further insight into the differences in field response mechanisms was determined by analyzing the field-dependent data via single peak fitting to extract information about the position and intensity of 111, 002, and 200 reflections using the lmfit python package.[18] Each reflection was modeled using a normalized Pseudo-Voigt peak shape with a linear background. See Figs. S2–S4 for representative peak-fit results.

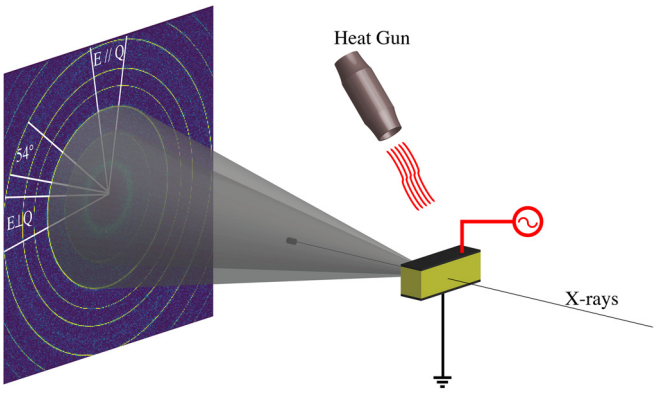

FIG. 1. Schematic representation of the experimental setup used to measure electric field dependent diffraction data at elevated temperature. Detector annotations indicate the regions of the detector used to determine angular dependent response phenomena.

Field-dependent peak center and intensity information were used to determine induced *hkl* dependent lattice strain and domain reorientation. Lattice strain was determined using

$$\varepsilon_{hkl} = \frac{d_{hkl}(E)}{d_{hkl}(E=0)} - 1, \tag{1}$$

where the lattice spacing at zero-field was used as the strain reference. The extent of domain reorientation was quantified using[19]

$$\eta_{002} = \frac{\frac{I_{002}}{I^R_{002}}}{\frac{I_{002}}{I^R_{002}} + 2 \times \frac{I_{200}}{I^R_{200}}} - \frac{1}{3}, \tag{2}$$

where I_{002} and I_{200} are the integrated intensities of the 002 and 200 tetragonal reflections, respectively. I^R_{002} and I^R_{200} represent the integrated intensities of the 002 and 200 tetragonal reflections of an unpoled specimen. Estimated uncertainties in the peak position and intensity (95th confidence interval) to ε_{hkl} and η_{002} were propagated using the Uncertainties python package.[20]

The application of strong electric fields induces extensive domain switching and 111 lattice strain. Figure 3 compares the measured 111 lattice strain, and the fraction of domains switched at RT and 56 °C. These data suggest that an increase in temperature results in a slight reduction in both the extent of domain reversal and lattice strain. Observing a reduction in the maximum achieved domain alignment and similar remnant domain alignment at 56 °C is counter-intuitive, considering that poling at elevated temperatures enhances the electromechanical response of 60BCT.[21] However, prolonged poling might enhance the remnant domain alignment. Increasing measurement temperature has been shown to decrease the coercive field (E_c) in soft-doped PZT.[22] The field dependence in η_{002} in Fig. 3 indicates that the E_c is reduced at 56 °C, which would increase the E_{max}/E_c and should provide a greater driving force for domain alignment. Ching-Chang *et al.* used temperature-dependent *in situ* XRD to determine an 0.45 eV activation energy for DWM in Nb-doped PZT (56/44).[23] A low activation energy would imply that a constant magnitude of the applied electric fields would induce a greater extent of domain alignment at elevated temperatures than room temperature. Instead, the reduction in η_{002} indicates that the energetics underpinning DWM in 60BCT are more complicated than soft-doped PZT.

Prior work by Tutuncu *et al.* and Manjón-Sanz *et al.* determined that the extent of ferroelastic DWM increased with decreasing c/a as BCT content approached the MPB.[24,25] Tutuncu suggested that the reduction in c/a relieved intergranular constrained that might pin ferroelastic DWM. In this work, increasing temperature to 56 °C reduces c/a from 1.006 to 1.005. The subsequent reduction in c/a should enhance the maximum achieved domain alignment (assuming that c/a is a metric to gauge the propensity for pinning ferroelastic DWM). A smaller c/a at elevated temperature coincided with a reduction in η_{002},

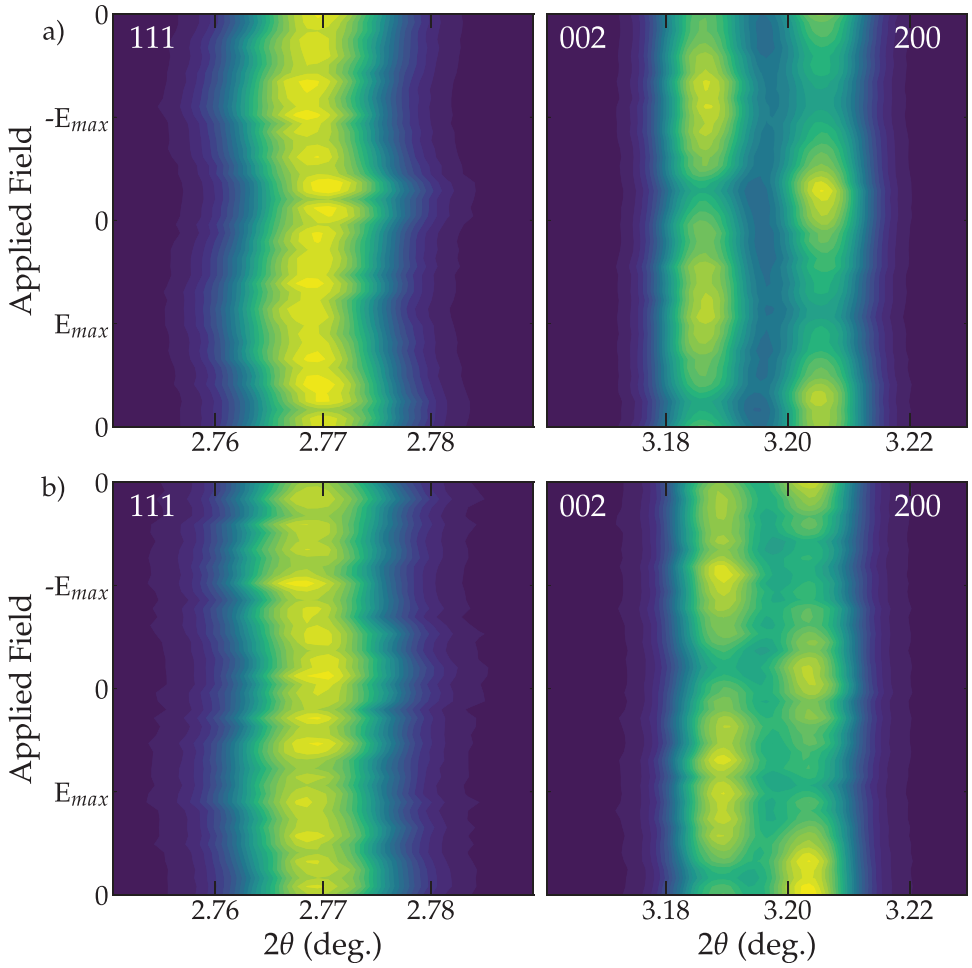

FIG. 2. Electric field dependence of the 111 (left) and 002/200 (right) diffraction data measured at RT (a) and 56 °C (b) for scattering vectors aligned in the field direction.

indicating that the underlying increase in DWM previously reported originates from more complex processes. Unlike PZT, the composition range of the MPB in BZT-BCT is strongly dependent on temperature. Reducing the BCT content has the unintended consequence of changing the proximity to the T-O PPB.[26] Similar to an MPB, PPBs have a complex energy landscape where multiple phases have comparable free-energies. Observing less domain alignment at 56 °C indicates that DWM is less favorable farther from the MPB or PPB.[15]

Prototypical polarization rotation or extension field-response mechanisms are characterized by the observation of lattice strain along a non-polar or polar axis, respectively.[26] The lattice strain evolution in 60BCT exhibits both rotation and extension characteristics with a high 111 and non-negligible 002/200 lattice strains. We note that Tutuncu *et al.* determined the ferroelastic switching high-field strain response mechanism in 60BCT.[24] However, the 002/220 lattice response in 60BCT is more intricate. The field-dependent evolution in the 002/200 lattice strain evidences that the underlying c/a ratio decreases with an increase in electric field (see Fig. S5). The magnitude of the c/a contraction is also strongly dependent on the polar axis orientation with respect to the applied field. Figure 4 compares the angular dependence of the change in c/a (Δc/a) measured at RT and 56 °C. See Fig. S6 for the absolute change in c/a. The reduction in c/a is nearly identical parallel and perpendicular to the applied field. However, grains with their [111] aligned with the electric field direction exhibit the most significant contraction in c/a. The observed reduction in c/a is more pronounced at RT (0.08%) than 56 °C (0.03%). Ehmke *et al.*[27] attributed the reduction in c/a with the increase in applied fields to the change in stress state with 90° switching inducing compressive stress in the field direction. Subsequent intragranular interactions between neighboring grains result in the development of tensile stresses orthogonal to the applied field. This explanation does not account for observing a larger Δc/a for grains oriented with their [111] aligned with the applied field. Ehmke *et al.* reported that the elastic moduli (E) in 60BCT decreases from 135 GPa at room temperature to 122 (GPa) at 50 °C.[14] The slight reductions in E and η_{002} would suggest that the intragranular interactions should result in a similar c/a behavior between RT and 56 °C. Observing a more pronounced reduction in c/a at RT than 56 °C indicates that the underlying micromechanical evolution is more complex.

The evolution of the stress state within each grain is a complex function of *E*, grain orientation, ferroelastic DWM, and propensity for

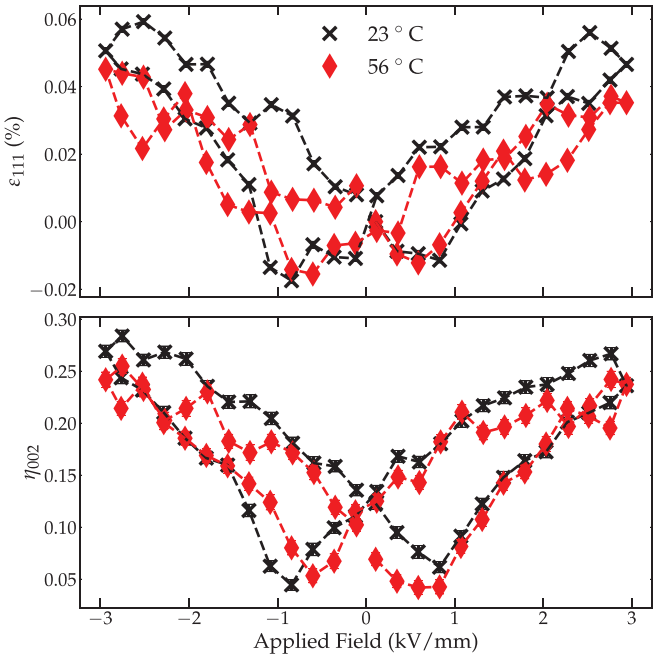

FIG. 3. Electric field dependence of ε_{111} (top) and η_{002} measured at RT and 56 °C. We note that these data represent the response in the field direction. Error bars represent the 95th confidence interval and in some cases are smaller than the symbols.

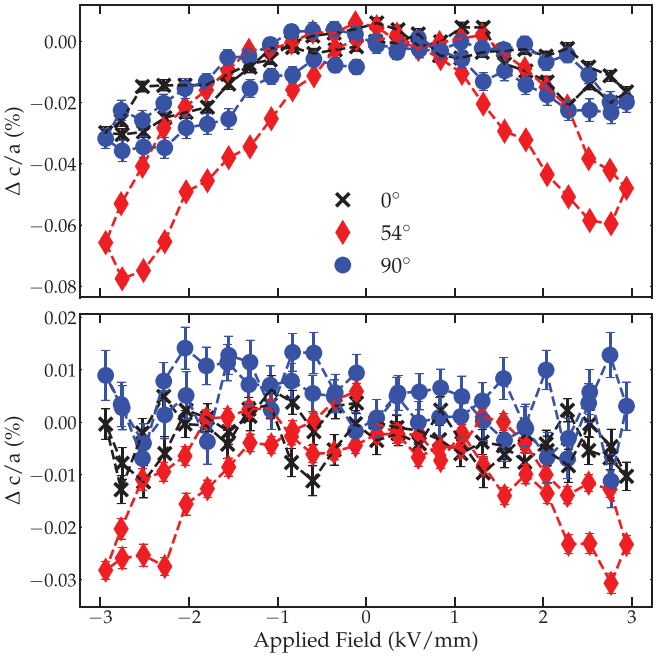

FIG. 4. Electric field dependence of the change in c/a for grain with their 002/200 grains oriented 0°, 45°, and 90° to the electric field direction measured at RT (top) and 56 °C (bottom). Dashed lines are shown for visual reference. Error bars represent the 95th confidence interval and in some cases are smaller than the symbols.

field-induced transitions with applied fields.[28,29] Grains with their [111] oriented in the field direction are in a special configuration where all 00l variants are equally favorable.[30] Application of electric fields along the non-polar direction induces substantial lattice strain (see Fig. 3) through piezoelectric shear.[31,32] The similarity of ε_{111} observed at RT and 56 °C suggests that the differences in measurement temperature do not strongly impact the magnitude of the macroscopic strain response. Therefore, the differences in the c/a for [111] oriented grains could arise from changing the underlying energetics of the system by increasing the ΔT from the T-O PPB. Flattening of the free-energy landscape near phase boundaries facilitates field-induced polymorphic transitions[33] and easy polarization rotation through monoclinic phases.[34] The orientation of each grain within the polycrystalline sample impacts the phase selection, with [111] oriented grains preferring a rhombohedral distortion.[35,36] We note that no evidence for a polymorphic transition is observed. Instead, we attribute the enhanced reduction in c/a for [111] oriented grains to the development of a complex stress state that is more pronounced at RT due to the enhanced polarization rotation near to the T-O PPB. These data evidence how the thermal evolution of the free-energy landscape underpins DWM and field-induced transitions.

We have investigated the effects of temperature on the field-response mechanism in BZT-60BCT using *in situ* x-ray diffraction. These results indicate that both the extent of domain wall alignment and the magnitude of 111 lattice strain are reduced at elevated temperatures. The increasing temperature profoundly impacted the evolution of the angular dependence of the 002/200 lattice strain. We attribute the observed reduction in c/a for grains with their [111] oriented in the field direction to the high piezoelectric shear response associated with polarization rotation. The apparent effects of polarization rotation on the 002/200 lattice stain are minimized at higher temperatures, indicating that the proximity of BZT-BCT to the T-O phase boundary underpins the reduction in the extent of domain alignment and anomalous reduction in c/a.

See the supplementary material for a summary of the angular dependent, representative fits, angular dependent lattice stain, and absolute change in c/a.

This work was supported by the U.S. National Science Foundation Grant No. DMR 0805022. Use of the Advanced Photon Source was supported by the U. S. Department of Energy, Office of Science, Office of Basic Energy Sciences, under Contract No. DE-AC02-06CH11357. This manuscript has been authored by UT-Battelle, LLC under Contract No. DE-AC05-00OR22725 with the U.S. Department of Energy.

DATA AVAILABILITY

The data that support the findings of this study are available from the corresponding author upon reasonable request.

REFERENCES

[1]B. Jaffe, W. R. Cook, and H. Jaffe, *Piezoelectric Ceramics* (Academic Press, London/New York, 1971), p. 317.
[2]J. Rödel, K. G. Webber, R. Dittmer, W. Jo, M. Kimura, and D. Damjanovic, J. Eur. Ceram. Soc. **35**, 1659 (2015).
[3]N. J. Donnelly, T. R. Shrout, and C. A. Randall, J. Am. Ceram. Soc. **90**, 490 (2007).
[4]H. Kungl and M. J. Hoffmann, Acta Mater. **55**, 5780 (2007).

[5]J. Rödel, W. Jo, K. T. P. Seifert, E.-M. Anton, T. Granzow, and D. Damjanovic, J. Am. Ceram. Soc. **92**, 1153 (2009).
[6]J. Rödel and J.-F. Li, MRS Bull. **43**, 576 (2018).
[7]Y. Saito, H. Takao, T. Tani, T. Nonoyama, K. Takatori, T. Homma, T. Nagaya, and M. Nakamura, Nature **432**, 84 (2004).
[8]M. Acosta, N. Novak, V. Rojas, S. Patel, R. Vaish, J. Koruza, G. A. Rossetti, and J. Rödel, Appl. Phys. Rev. **4**, 041305 (2017).
[9]J. Gao, X. Ke, M. Acosta, J. Glaum, and X. Ren, MRS Bull. **43**, 595 (2018).
[10]C.-C. Huang and D. P. Cann, J. Appl. Phys. **104**, 024117 (2008).
[11]D. Xue, P. V. Balachandran, R. Yuan, T. Hu, X. Qian, E. R. Dougherty, and T. Lookman, Proc. Natl. Acad. Sci. U. S. A. **113**, 13301 (2016).
[12]D. Hou, T. M. Usher, H. Zhou, N. Raengthon, N. Triamnak, D. P. Cann, J. S. Forrester, and J. L. Jones, J. Appl. Phys. **122**, 064103 (2017).
[13]W. Liu and X. Ren, Phys. Rev. Lett. **103**, 257602 (2009).
[14]M. C. Ehmke, F. H. Schader, K. G. Webber, J. Rödel, J. E. Blendell, and K. J. Bowman, Acta Mater. **78**, 37 (2014).
[15]M. Acosta, N. Novak, W. Jo, and J. Rödel, Acta Mater. **80**, 48 (2014).
[16]M. C. Ehmke, S. N. Ehrlich, J. E. Blendell, and K. J. Bowman, J. Appl. Phys. **111**, 124110 (2012).
[17]J. Kieffer and D. Karkoulis, J. Phys.: Conf. Ser. **425**, 202012 (2013).
[18]M. Newville, R. Otten, A. Nelson, A. Ingargiola, T. Stensitzki, D. Allan, A. Fox, F. Carter, Michał, D. Pustakhod, Lneuhaus, S. Weigand, R. Osborn, Glenn, C. Deil, Mark, A. L. R. Hansen, G. Pasquevich, L. Foks, N. Zobrist, O. Frost, A. Beelen, Stuermer, Kwertyops, A. Polloreno, S. Caldwell, A. Almarza, A. Persaud, B. Gamari, and B. F. Maier, https://zenodo.org/record/4516651#.YOSx2C1h2c5 (2021).
[19]J. L. Jones, E. B. Slamovich, and K. J. Bowman, J. Appl. Phys. **97**, 034113 (2005).
[20]E. O. Lebigot, *Uncertainties: A Python Package for Calculations With Uncertainties*, https://uncertainties-python-package.readthedocs.io/en/latest/# (2021).
[21]B. Li, J. E. Blendell, and K. J. Bowman, J. Am. Ceram. Soc. **94**, 3192 (2011).
[22]A. B. Kounga, T. Granzow, E. Aulbach, M. Hinterstein, and J. Rödel, J. Appl. Phys. **104**, 024116 (2008).
[23]C. C. Chung, C. M. Fancher, C. Isaac, J. Nikkel, E. Hennig, and J. L. Jones, J. Am. Ceram. Soc. **100**, 4352 (2017).
[24]G. Tutuncu, B. Li, K. J. Bowman, and J. L. Jones, J. Appl. Phys. **115**, 144104 (2014).
[25]A. Manjón-Sanz, C. M. Culbertson, D. Hou, J. L. Jones, and M. R. Dolgos, Acta Mater. **171**, 79 (2019).
[26]D. Damjanovic, Appl. Phys. Lett. **97**, 062906 (2010).
[27]M. C. Ehmke, N. H. Khansur, J. E. Daniels, J. E. Blendell, and K. J. Bowman, Acta Mater. **66**, 340 (2014).
[28]M. Hinterstein, K. Y. Lee, S. Esslinger, J. Glaum, A. J. Studer, M. Hoffman, and M. J. Hoffmann, Phys. Rev. B **99**, 174107 (2019).
[29]J. E. Daniels, M. Majkut, Q. Cao, S. Schmidt, J. Wright, W. Jo, and J. Oddershede, Sci. Rep. **6**, 22820 (2016).
[30]S. Wada, K. Yako, H. Kakemoto, T. Tsurumi, and T. Kiguchi, J. Appl. Phys. **98**, 014109 (2005).
[31]M. Davis, M. Budimir, D. Damjanovic, and N. Setter, J. Appl. Phys. **101**, 054112 (2007).
[32]M. E. Manley, D. L. Abernathy, R. Sahul, D. E. Parshall, J. W. Lynn, A. D. Christianson, P. J. Stonaha, E. D. Specht, and J. D. Budai, Sci. Adv. **2**, e1501814 (2016).
[33]M. Hinterstein, J. Rouquette, J. Haines, P. Papet, M. Knapp, J. Glaum, and H. Fuess, Phys. Rev. Lett. **107**, 077602 (2011).
[34]B. Noheda, D. E. Cox, G. Shirane, S.-E. E. Park, L. E. Cross, and Z. Zhong, Phys. Rev. Lett. **86**, 3891 (2001).
[35]G. Esteves, C. M. Fancher, S. Röhrig, G. G. A. Maier, J. L. Jones, and M. Deluca, Acta Mater. **132**, 96 (2017).
[36]J. Paul, T. Nishimatsu, Y. Kawazoe, and U. V. Waghmare, Phys. Rev. B **80**, 024107 (2009).